Spatial and temporal variability of freshwater discharge into the Gulf of Alaska

Citation	Hill, D. F., Bruhis, N., Calos, S. E., Arendt, A., & Beamer, J. (2015). Spatial and temporal variability of freshwater discharge into the Gulf of Alaska. Journal of Geophysical Research: Oceans, 120(2), 634-646. doi:10.1002/2014JC010395
DOI	10.1002/2014JC010395
Publisher	American Geophysical Union
Version	Version of Record
Terms of Use	http://cdss.library.oregonstate.edu/sa-termsofuse

Oregon State
UNIVERSITY

Spatial and temporal variability of freshwater discharge into the Gulf of Alaska

## D. F. Hill[1], N. Bruhis[2], S. E. Calos[3], A. Arendt[4], and J. Beamer[5]

[1]School of Civil and Construction Engineering, Oregon State University, Corvallis, Oregon, USA, [2]Decagon Devices, Pullman, Washington, USA, [3]School of Engineering and Applied Science, University of Virginia, Charlottesville, Virginia, USA, [4]Geophysical Institute, University of Alaska Fairbanks, Fairbanks, Alaska, USA, [5]Water Resources Engineering, Oregon State University, Corvallis, Oregon, USA

Abstract A study of the freshwater discharge into the Gulf of Alaska (GOA) has been carried out. Using available streamgage data, regression equations were developed for monthly flows. These equations express discharge as a function of basin physical characteristics such as area, mean elevation, and land cover, and of basin meteorological characteristics such as temperature, precipitation, and accumulated water year precipitation. To provide the necessary input meteorological data, temperature and precipitation data for a 40 year hind-cast period were developed on high-spatial-resolution grids using weather station data, PRISM climatologies, and statistical downscaling methods. Runoff predictions from the equations were found to agree well with observations. Once developed, the regression equations were applied to a network of delineated watersheds spanning the entire GOA drainage basin. The region was divided into a northern region, ranging from the Aleutian Chain to the Alaska/Canada border in the southeast panhandle, and a southern region, ranging from there to the Fraser River. The mean annual runoff volume into the northern GOA region was found to be 792 ± 120 km³ yr^{-1}. A water balance using MODIS-based evapotranspiration rates yielded seasonal storage volumes that were consistent with GRACE satellite-based estimates. The GRACE data suggest that an additional 57 ± 11 km³ yr^{-1} be added to the runoff from the northern region, due to glacier volume loss (GVL) in recent years. This yields a total value of 849 ± 121 km³ yr^{-1}. The ease of application of the derived regression equations provides an accessible tool for quantifying mean annual values, seasonal variation, and interannual variability of runoff in any ungaged basin of interest.

1. Introduction

Alaska, USA and northwestern Canada, both of which border the Gulf of Alaska (GOA), present a hydrological and nearshore oceanographic challenge. The region experiences extreme values of precipitation, temperature, and topographic elevation, as well as extreme spatial gradients in these quantities. In addition, glacier mass changes contribute a strong runoff signal, and weather and streamflow data are comparatively sparse. The temporal and spatial distributions of coastal freshwater discharge represent the hydrological response of this complex system to its complex forcing. Estimates of coastal freshwater discharge into the GOA are necessary for a variety of stakeholders. Freshwater fluxes play a key role in controlling nearshore salinity and temperature fields and resultant oceanographic circulations. The coastal waters of the GOA represent important habitat for a wide variety of marine organisms [*Etherington et al.*, 2007] and these water column properties play a role in controlling observed biological patterns.

The GOA region is generally undersampled, when it comes to freshwater resources. Figure 1 illustrates the major watersheds in the area, all of which are gaged. Even these "major" watersheds are quite small, by the standards of the contiguous U.S. This is due to the extreme topographic relief which divides the entire GOA drainage into thousands of small drainages. The GOA watershed shown in Figure 1 was delineated from the GTOPO30 (Global 30 Arc-Second Elevation) digital elevation model with the coastal boundary running from the Fraser River to the tip of the Aleutian chain. The six watersheds shown in Figure 1 drain approximately 50% of the entire GOA drainage. The remaining flow occurs in a highly distributed fashion that is better represented as a line source rather than a point source [*Royer*, 1982]. The number of drainages coupled with remote terrain and harsh winter climate means that a field measurement-based approach to water resource
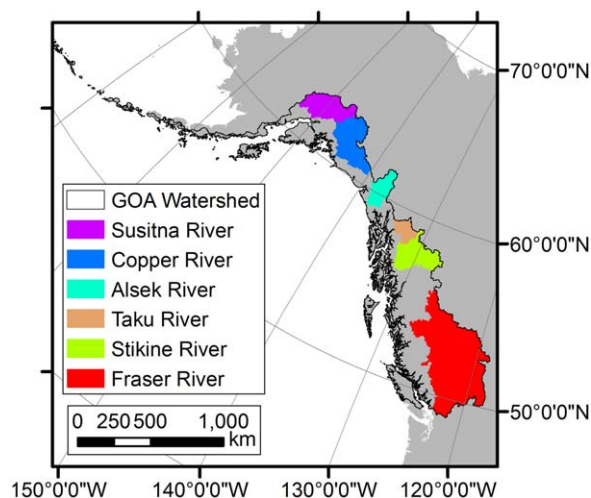
Figure 1. Overview map of the GOA region from the Aleutian Chain to the Fraser River. Black line shows the entire GOA drainage, and colored regions indicate major watersheds.

monitoring is not a complete solution. To complement stream gaging efforts, a modeling program is therefore required.

A number of previous studies have proposed estimates of coastal freshwater discharge (FWD), with particular emphasis on the GOA drainage. *Royer* [1982] used a hydrology model driven by precipitation and air temperature data from low elevation weather stations to arrive at an annually averaged value of 725 km^3 yr^{-1}. This value was expected to be an underestimate due to a lack of precipitation measurements at high elevations [*Royer*, 1982]. The equivalent mean annual runoff depth (runoff volume divided by drainage area) was 2.26 m. *Wang et al.* [2004] estimated a mean annual GOA FWD of 728 km^3 yr^{-1} using weather station and reanalysis data from 1958 to 1998 on a nominal 2° grid ($\sim$100 km × 200 km) and temperature-index simulations of snow and ice melt. The GOA watershed used by *Wang et al.* [2004], determined from a digital elevation model, covered a larger drainage area than used by *Royer* [1982] and therefore yields a lower FWD estimate per unit area. The mean annual runoff depth found by *Wang et al.* [2004] was 1.55 m. There have been fewer studies of the coastal discharge of British Columbia. *Morrison et al.* [2012] estimated a mean annual FWD of $\sim$550 km^3 yr^{-1} for a watershed ranging from the Nass River in the north to the Fraser River in the south. This runoff corresponds to a runoff depth of 1.16 m.

The studies described above included the effects of glaciers on seasonal runoff, but did not consider runoff due to glacier volume loss (GVL). *Royer and Grosch* [2006] noted that increases in GVL from Alaska glaciers [e.g., *Gardner et al.*, 2013] are likely evidenced by changes in oceanographic temperature and salinity in the northern Gulf of Alaska. Therefore, *Neal et al.* [2010] incorporated GVL estimates of *Arendt et al.* [2002] into their GOA discharge estimates. The nonglacial component of their estimates came from overlaying the PRISM (Parameter-elevation Regression on Independent Slopes Model) climatology [*Daly et al.*, 1994] on the ungaged watersheds lying between the major (gaged) watersheds in the GOA drainage. They estimated a mean annual discharge of 870 km^3 yr^{-1} into the GOA, with approximately 10% of that coming from GVL, but were unable to quantify interannual variability in the discharge. The equivalent runoff depth was 2.07 m with GVL included and 1.86 m with GVL excluded.

The goal of the present study is to continue to improve the spatiotemporal resolution and the accessibility and utility of estimates of GOA freshwater discharge. The works cited above provide an incomplete understanding of this discharge. The works of *Royer* [1982] and *Royer and Grosch* [2006] provide monthly resolution, which is suitable for seeing annual and interannual variation, but only a basin-integrated value (i.e., basin-scale ($\sim$1000 km) spatial resolution). Regional circulation studies of the GOA [*Hermann and Stabeno*, 1996; *Hermann et al.*, 2002] require discharge as a boundary condition. These studies have tended to simply distribute the runoff predicted by *Royer* [1982] and *Royer and Grosch* [2006] uniformly along their coastline boundaries, though *Hermann et al.* [2002] did augment the inflow with point-source contributions from the Copper and Susitna Rivers.

While the optimal grid size of the boundary forcing remains an open question, it should be commensurate with or less than the length scale of the features of interest. As one example, *Marsh et al.* [2010] used high spatial resolution estimates of the runoff from the Greenland ice sheet coupled to a high-resolution ocean circulation model, showing that the high resolution was necessary to resolve the structure of the boundary currents. Along the GOA coastline, 30 km eddies are prominent features [*Hermann and Stabeno*, 1996], suggesting a runoff product there with a grid size of 30 km or less. For more local, fjord-scale circulation studies, the relevant length scale may be the width, often less than 10 km.

We note that excellent databases of continental discharge do exist [*Dai and Trenberth*, 2002] and are candidates for providing boundary conditions for circulation studies. The spatial resolution is 1°, which is roughly equivalent to 55 × 110 km at 60° latitude. This is inadequate for local (fjord-scale) studies and may also be inadequate for regional GOA shelf simulations where 30 km eddies are expected. A larger concern is that their methods for scaling up observed river flow to unmonitored regions are not well validated in regions with extreme orographic effects in precipitation, such as coastal Alaska.

To accomplish this study's goal, regression equations for the entire region are developed. This approach involves regressing measured discharge against watershed characteristics such as area, elevation, and land cover; and weather characteristics such as mean monthly temperature and precipitation. The resulting regression coefficients are then used to predict discharge in ungaged basins. The method is a potentially powerful tool, especially in regions where the detailed data required to run complex physical models are not available. As examples, *Curran et al.* [2003] and *Wiley and Curran* [2003] describe equations for the estimation of flow-duration statistics and peak flood flows in Alaska, respectively. As a preliminary step to this phase of the study, new high-resolution (2 km) gridded precipitation and temperature data sets for Alaska and northwestern Canada have been developed. These data sets have been archived and made publicly available by the National Climatic Data Center at ftp://ftp.ncdc.noaa.gov/pub/data/gridded-nw-pac.

Given the complexity of the GOA hydrological system, there is a need for validation of discharge estimates using independent data sets. For example, discharge of freshwater into the Gulf of Alaska makes its way into the Alaska Coastal Current and travels westward along the Gulf of Alaska shelf. *Weingartner et al.* [2005] examined oceanographic and meteorological data to estimate the freshwater budget of this current, arriving at a value of 880 km^3 yr^{-1}, which agrees well with the discharge estimates of *Neal et al.* [2010] that include the effects of GVL. Here, satellite gravimetric data from the NASA/DLR Gravity Recovery and Climate Experiment (GRACE) are used as an independent validation of water balance calculations based on the modeled FWD. GRACE data provide direct measurement of variations in water mass at high temporal (~10 days) but coarse spatial resolution. The spatial resolution of the GRACE solutions in Alaska is equivalent to a 300 km Gaussian spatial smoothing filter *Luthcke et al.* [2013]. These data are, therefore, well suited for validation of large-scale changes in hydrology [*Ramillien et al.*, 2008].

2. Methods

2.1. Water Balance
Coastal FWD is the runoff *R* from a coastal watershed and is one component of the water balance equation

$$\frac{dS}{dt} = P - R - ET. \tag{1}$$

In this equation, *S* is the volume of water stored in the watershed, and the precipitation input *P*, the runoff *R*, and the evapotranspiration *ET* are all taken to be in rate form. The main objective of this paper is the determination of *R*, but all three terms on the right-hand side will be needed in order to facilitate comparisons of storage changes with those from the GRACE data. The following sections explain how the various components of equation (1) were determined.

2.2. Monthly Precipitation and Temperature Grids
2.2.1. Weather Station Data
The general domain of interest consists of portions of the state of Alaska, USA and British Columbia (BC) and the Yukon Territory (YT) in Canada. Weather data for Alaska were obtained from the National Climatic Data Center (http://www.ncdc.gov). For Canada, data were obtained from the National Climate Data and Information Archive (http://climate.weatheroffice.gc.ca). For this study, only stations reporting mean monthly data during the period 1961–2009 were considered. Of these, many were temporary installations yielding data for only a very short period. Stations reporting fewer than 36 (not necessarily consecutive) months were not included in the analysis.

In the calculation of gridded anomalies (discussed later), nonphysical oscillations would occasionally result from strong spatial gradients between adjacent stations. To resolve this, a "distance-based" filter was applied whereby the closest pair of stations in the data set was identified, one station from the pair was removed, and the process was repeated with the new ensemble of stations. The final data set for Alaska
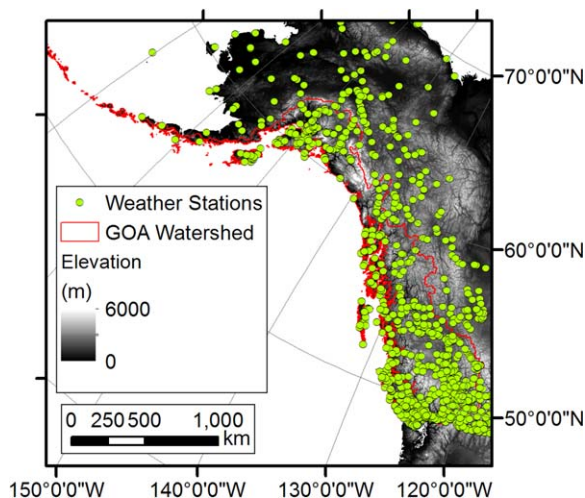
Figure 2. Topographic relief of Alaska, British Columbia, and the Yukon Territory, and locations of weather stations.

contained 200 stations for precipitation and 150 stations for temperature. For Canada, 500 stations each were retained for precipitation and temperature. Figure 2 displays station locations corresponding to this finalized data set, in addition to the topographic relief of the region.

2.2.2. Climatological Norms

Climatological norms, representing 30 year averages, for the region were obtained from the PRISM (http://www.prism.oregonstate.edu) model [*Daly et al.*, 1994, 2008]. PRISM is a model that uses regression equations to interpolate temperature and precipitation as a function of local topography [*Daly et al.*, 1994, 2008]. Details of weather station and snow course data used for the Alaska region are in *Simpson et al.* [2005]. Many traditional temperature and precipitation gridding approaches (e.g., kriging) perform poorly in areas of significant topographic relief, where orographic effects control weather patterns. The PRISM model addresses this by considering the elevation and aspect of each grid cell. The regression equations are developed to prioritize weather stations that have topographic characteristics that are similar to the grid cell of interest. *Simpson et al.* [2005] recently compared the PRISM data with data generated by the Alaska Geospatial Data Clearinghouse (AGDC) and concluded that the PRISM data provide the best available spatial coverage of long-term mean monthly surface temperature and precipitation.

2.2.3. Calculation of Station Anomalies

To determine the monthly weather grids, a "Delta" approach was adopted [*Jones*, 1994; *New et al.*, 2000; *Fowler et al.*, 2007; *Mosier et al.*, 2013]. This two-step method consists of first computing an anomaly field, which quantifies the deviation of weather conditions (for a given time period; typically monthly) from a climatological norm. Second, this field is combined with the norm itself in order to obtain a gridded estimate of the weather conditions for that time period. The inherent assumption of this method is that the spatial derivative of the anomaly field is much less than the spatial derivative of the normal field [*Mitchell and Jones*, 2005]. Creating a gridded time series of temperature or precipitation directly from station data is possible, but is complicated by the bias that most weather stations are at low elevations. In mountainous terrain, where precipitation has strong spatial variations, the direct interpolation of weather data from sparse, low-lying stations to a dense grid of high-elevation cells will generally be unsatisfactory.

For the first step, for each month in the period of 1961–2009, anomalies were computed for both precipitation and temperature at all reporting station locations. Note that "reporting stations" are a subset of the final station data sets described above. For Alaska, on average, 75 stations would report precipitation data in a given month and 55 stations would report temperature data. For Canada, on average, 170 stations would report data, both for precipitation and for temperature. In the case of precipitation, a proportional anomaly was computed as the ratio of a station data value to the PRISM data value interpolated to that location. Proportional anomalies were used to avoid the nonphysical scenario of having negative rainfall values in the final grid. In the case of temperature, an absolute anomaly was computed as the difference between a station data value and the PRISM data value interpolated to that location.

2.2.4. Calculation of Gridded Results

The anomaly values at the station locations were next interpolated back onto the regular grid of the original PRISM data (2 km resolution). For this step, a spline with tension method [*Wessell and Bercovici*, 1998] was used. The tension parameter (ranging between 0 and 1) helps to suppress spurious oscillations and was selected to be 0.8. To arrive at this tension parameter, leave-one-out cross-validation calculations were carried out for a wide range of tension values, for one sample month. The RMSE between the reported station data and the station data computed at the missing ("left out") station decreased with increasing tension. Too much tension, however, renders the interpolation purely linear [*Wessell and Bercovici*, 1998]. A value of

0.8 was, therefore, chosen as a compromise between reducing error and keeping physically smooth variation. For the precipitation grids, any interpolated anomaly values less than zero were set to be zero, again to prevent negative precipitation values. This is, in ways, similar to the method of *Mitchell and Jones* [2005] who inserted "dummy" anomalies of zero in regions of few stations. The anomaly and the PRISM grids were then combined (multiplied in the case of precipitation, added in the case of temperature) in order to obtain the high-resolution gridded precipitation and temperature for the month and year in question.

2.3. Discharge From Regression Analysis

The equations of *Wiley and Curran* [2003] and *Curran et al.* [2003] are useful in predicting peak flows and information about exceedance probabilities, but they have no connection to the present and recent weather. In order to predict the flow for a given month (Q_i, $i = 1 \ldots 12$), the flow was modeled as

$$Q_i = A x_1^{a_1} x_2^{a_2} x_3^{a_3} \ldots, \tag{2}$$

where x denotes an explanatory variable and a denotes a regression coefficient. This equation is equivalent to
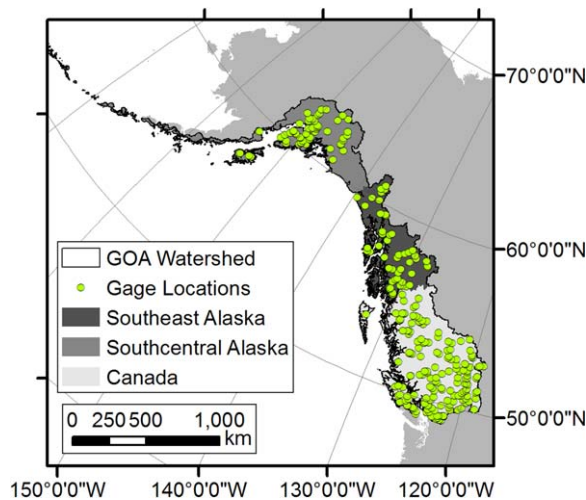
$$\log (Q_i) = \log (A) + a_1 \log (x_1) + a_2 \log (x_2) + a_3 \log (x_3) \ldots, \tag{3}$$

so, using log-transformed variables, it is immediately possible to use multiple linear regression.

Several data sets were required to perform the regression analysis. First, streamflow data between 1961 and 2009 were obtained for all unregulated watersheds from the U.S. Geological Survey (U.S. sites) and Environment Canada (Canadian sites). Here "unregulated" refers to the lack of a dam or substantial diversions upstream. Many of these stations were temporary installations with very short records. Only stations with at least 36 (not necessarily consecutive) months of data were retained. These stations are illustrated in Figure 3. Next, physical data relating to the gaged watersheds were required. These data included area, mean elevation, slope, land cover, etc. For the U.S. sites, these data were available in the reports by *Wiley and Curran* [2003] and *Curran et al.* [2003]. For the Canadian sites, these data were obtained from the GTOPO30 DEM and the North American Land Change Monitoring System's (NALCMS) Land Cover 2005 map. Finally, weather data for each gaged watershed were required and were obtained from the downscaled grids described immediately above.

Too much spatial aggregation can produce unsatisfactory regression equations, as regional hydrologic variations are not preserved. *Curran et al.* [2003] used seven subregions to group together hydrologically similar watersheds over the entire state of Alaska. As Figure 3 illustrates, three subregions were used for the GOA drainage being studied. The southcentral and southeast Alaska regions generally follow the guidance provided by *Curran et al.* [2003]. Note that "southeast Alaska" here refers to the coastline extent. It is acknowledged that this region contains a portion of Canada that happens to drain to the southeastern Alaska coast. The final form of the regression equation was taken to be

$$Q = A D^{a_D} E^{a_E} P^{a_P} C^{a_C} T^{a_T} G^{a_G}. \tag{4}$$

In this equation, the discharge Q is in $m^3 \, s^{-1}$, the drainage area D is in km^2, the mean elevation E is in m, the precipitation P is in m (with a value of 1 added), the cumulative precipitation C since the start of the water year (1 October) is in m, the temperature T is in °C (with a value of 32 added), and the "percent snow and ice" (the NALCMS terminology) or "glacier" coverage G is in % (with a value of 1 added). The added offsets are simply to prevent taking the log of a number less than or equal to zero. It must be stressed that, in applying this equation to an ungaged watershed, the same units and the same offsets described here must be used. The obtained coefficients are provided in Table 1.

Figure 3. Map of streamflow gage locations and regions used for the purposes of aggregating records.

Table 1. Regression Coefficients for the Three Defined Regions[a]
Southeastern Alaska

Month	J	F	M	A	M	J	J	A	S	O	N	D
$\log_{10}(A)$	1.44	0.75	−1.68	−8.02	−13.8	−7.49	−3.06	−4.55	−4.16	−6.20	0.87	2.46
a_D	1.04	1.04	1.04	0.99	0.98	0.96	0.93	0.89	0.91	0.90	0.96	0.99
a_E	−1.58	−1.49	−1.29	−0.98	−0.05	0.55	0.65	0.19	−0.18	−1.16	−1.79	−1.94
a_P	0.20	0.29	0.50	0.19	0.12	−0.23	−0.01	0.23	0.33	0.01	−0.06	−0.11
a_C	0.54	0.53	0.35	0.51	0.79	0.87	0.69	0.46	0.63	0.13	0.14	0.17
a_T	0.41	0.60	1.88	5.57	7.51	2.45	−0.51	1.25	1.57	5.45	1.90	0.88
a_G	−0.02	−0.01	0.02	0.11	0.04	0.09	0.32	0.47	0.30	0.29	0.18	0.12

Southcentral Alaska

Month	J	F	M	A	M	J	J	A	S	O	N	D
$\log_{10}(A)$	−2.71	−2.81	−3.41	−4.62	−5.94	−3.87	−4.43	−8.30	−7.48	−8.09	−4.95	−2.90
a_D	1.00	1.02	1.03	1.01	0.97	0.97	1.07	1.10	1.06	1.01	1.00	0.95
a_E	−0.18	−0.24	−0.29	−0.42	0.18	0.76	0.68	0.53	0.34	0.10	−0.13	−0.26
a_P	0.06	−0.16	−0.21	−0.16	−0.07	−0.04	0.01	0.54	0.84	−0.05	−0.10	−0.19
a_C	0.71	0.85	0.78	0.70	0.50	0.67	0.80	0.73	0.62	0.07	0.06	0.09
a_T	0.43	0.47	0.93	2.10	2.31	−0.04	0.10	2.55	2.45	4.05	2.36	1.18
a_G	−0.01	−0.03	0.00	0.00	−0.07	0.01	0.16	0.17	0.05	0.16	0.15	0.16

Canada

Month	J	F	M	A	M	J	J	A	S	O	N	D
$\log_{10}(A)$	−2.98	−4.81	−8.53	−10.4	−9.29	−7.76	−4.70	−3.42	−2.52	−2.98	−3.23	−1.39
a_D	1.06	1.07	1.06	0.97	0.96	1.07	1.18	1.24	1.19	1.03	0.99	1.00
a_E	−0.71	−0.63	−0.41	−0.14	0.64	1.26	1.41	1.23	0.71	−1.21	−1.41	−1.61
a_P	0.06	0.00	0.44	0.46	0.32	0.22	0.37	0.54	0.64	−0.10	−0.05	0.00
a_C	1.33	1.31	1.05	0.76	0.80	1.18	1.42	1.48	1.39	0.13	0.10	0.07
a_T	1.30	2.26	4.29	5.33	3.25	0.64	−2.03	−2.88	−2.48	2.89	3.72	2.87
a_G	0.01	0.02	0.03	0.04	0.05	0.14	0.29	0.44	0.41	0.76	0.57	0.49

[a]Note that $\log_{10}(A)$ is shown instead of A for brevity.

The performance of the regression equations was assessed by comparing the predicted flow to the measured flow. Specifically, for each of the 12 months, all stations and all years in a given region were binned and the weighted mean absolute percent error (WMAPE) was computed for that month as

$$\text{WMAPE} = \frac{\sum_{i=1}^{n} m_i \left| \frac{c_i - m_i}{m_i} \right|}{\sum_{i=1}^{n}}, \tag{5}$$

where n is the number of station-year values, m is the measured flow, and c is the calculated flow. There was only minor variation in WMAPE over the 12 months of the year; average values were 28%, 34%, and 40% for the Southeast Alaska, Southcentral Alaska, and Canada regions. These numbers are consistent with typical errors found by *Curran et al.* [2003] and *Wiley and Curran* [2003].

Finally, the regression equations were applied to a network of ungaged watersheds delineated from the entire GOA drainage basin, as shown in Figure 4, for the period 1960–2009. Watershed physical and weather data for these watersheds were obtained as described above.

2.4. Evapotranspiration From MODIS

The methods above are adequate for predicting precipitation inputs and runoff outputs from the domain. In order to provide estimates of ΔS in the domain, estimates of ET at similar temporal and spatial resolutions are also required. Remote sensing is the most feasible means of estimating ET over large

Figure 4. Watershed delineation for the three principal regions in the GOA drainage basin.
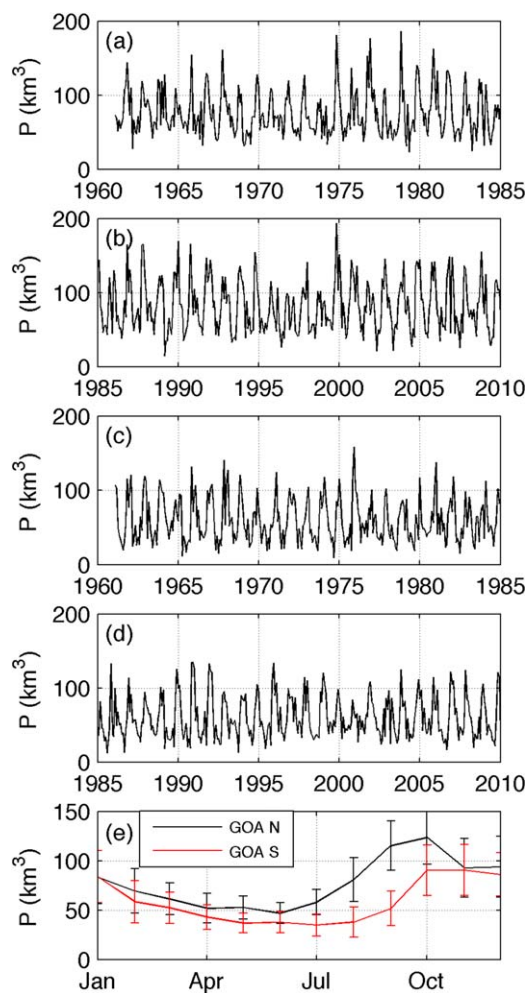
Figure 5. Monthly precipitation volumes from precipitation grids. (a and b) For the GOA N watershed and (c and d) for the GOA S watershed. (e) The mean of monthly values over the period 1960–2009; the bars show ± one standard deviation.

regions of mixed land cover type [*Glenn et al.*, 2010] and it is frequently used to develop regional ET estimates to construct water budget models [*Guerschman et al.*, 2009]. The Moderate-Resolution Imaging Spectraradiometer (MODIS) is one instrument that provides such ET estimates, using vegetation indices (VI) methods. A number of successful methods have been developed which combine MODIS VIs and ground-based weather station data to estimate ET in a wide variety of landscape types, including the arctic tundra and boreal forests of Alaska and northern Canada [*Mu et al.*, 2009; *Zhang et al.*, 2009], and in mixed landscapes at the continental [*Cleugh et al.*, 2007; *Guerschman et al.*, 2009] and global [*Mu et al.*, 2007] scales of measurement.

In this study, regional ET volumes were derived from the MODIS Global Evapotranspiration Project (MOD16) obtained from the Numerical Terradynamic Simulation Group at the University of Montana. The equations used to estimate MOD16 global ET are from *Mu et al.* [2011] which improved upon the old ET algorithm in *Mu et al.* [2007]. *Mu et al.* [2007] used MODIS land cover, albedo, leaf area index, an enhanced vegetation index and a daily meteorological reanalysis data set as inputs to map regional and global ET. *Mu et al.* [2011] improved the ET algorithm from *Mu et al.* [2007] by including calculations of soil heat flux, evaporation from plant canopy interception, and actual evaporation from moist soil surfaces in the daily ET formulation. *Mu et al.* [2011] applied this improved method to calculate ET globally and assessed the model results over 46 AmeriFlux eddy covariance flux towers with generally favorable agreement. Mean absolute error of the daily ET was 24.6% of the flux tower ET, within the 10–30% range of uncertainty in ET measurements.

Monthly MOD16 ET maps at 0.05° resolution were obtained for the period 2000–2009. These ET maps were clipped to the GOA drainage, and MODIS pixels with the following nonvegetated land cover types were omitted from the ET data set: barren areas, water bodies, snow and ice, and urban areas.
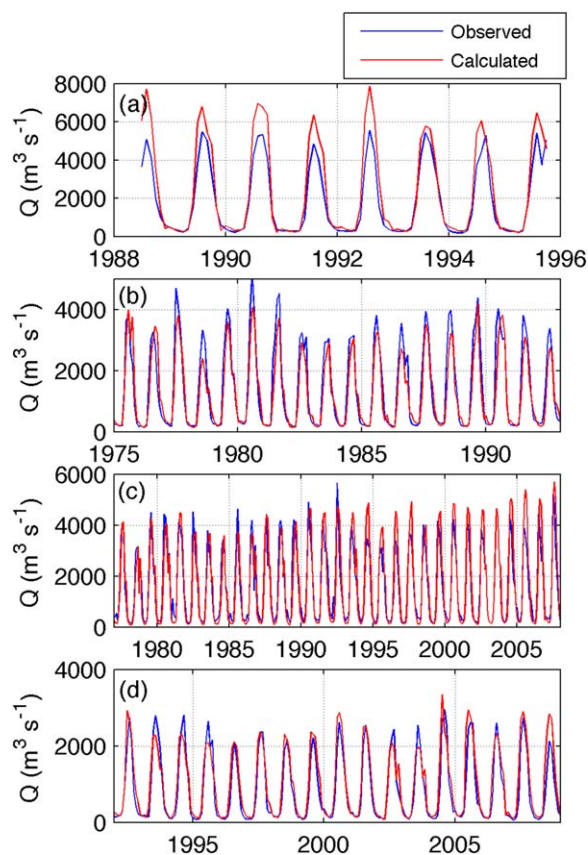
2.5. GRACE

Data from the NASA/DLR Gravity Recovery and Climate Experiment (GRACE) satellites were used as an independent validation of the GOA runoff estimates. GRACE measures time variations in Earth gravity resulting from changes in atmospheric and oceanic mass, Earth and ocean tides, mantle dynamics, and terrestrial hydrology including glaciers. Prior GRACE studies in the GOA region have focused on isolating the glacier mass balance signal, and have removed other components of mass change through incorporation of independent data sets or models [*Sasgen et al.*, 2012; *Jacob et al.*, 2012; *Arendt et al.*, 2013]. Here all elements of the water budget were retained within the GRACE signal to enable comparison with changes in water storage estimated from the regression analysis. The v08 high-resolution mascon solution from the NASA Goddard Space Flight Center was used. This solution does not correct for terrestrial water storage and precipitation, and is the GRACE product most closely aligned with the water balance estimates of this study [*Luthcke et al.*, 2013]. This GRACE solution provides a measure of the time-averaged storage of mass within 1° × 1° equal-area (approximately 12,390 km^2) mass concentration (mascon) grids, during approximately 10 day sampling

Figure 6. Observed and predicted hydrographs for the (a) Copper (USGS 15215000), (b) Susitna (USGS 15294350), (c) Stikine (USGS 15024800), and (d) Alsek (USGS 15129000) Rivers.
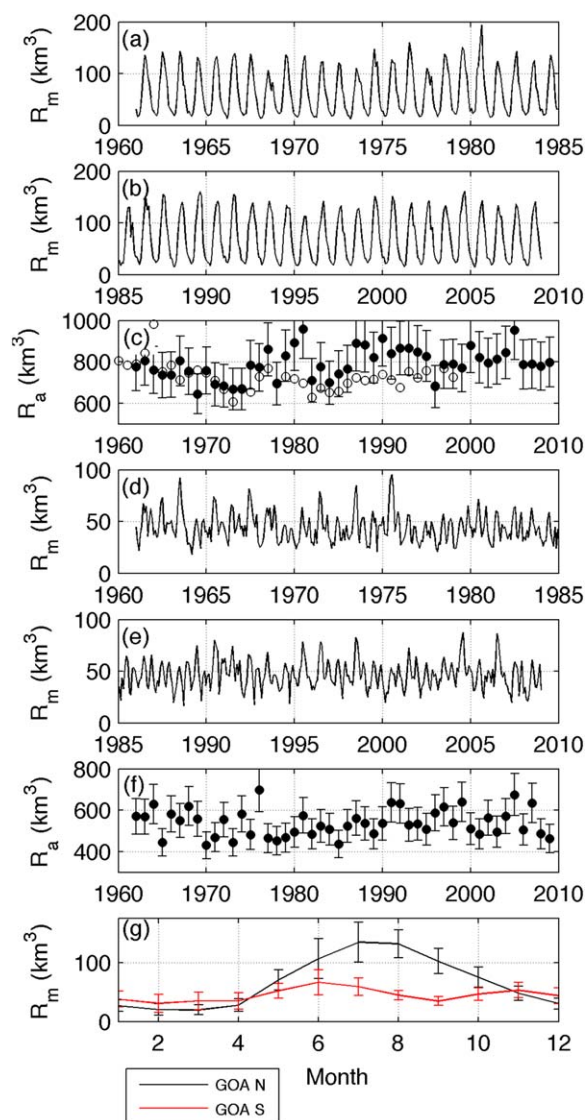
intervals. The total mass storage at each time interval was determined through summation of all mascons that intersect the GOA N watershed polygon.

Because GRACE data are time averages over multiple days, whereas modeled water balances represent total changes every month, it is necessary to resample the modeled time series to correctly align the sampling periods. To do this, the monthly data were interpolated using a cubic spline function, and then total and time-averaged accumulation values were calculated, expressed as mass rates per day, following *Swenson and Wahr* [2006]. For the GRACE data, the first difference of the mass time series was calculated to determine changes in storage from one time interval to the next, and then divided by the time interval of the observation. Total changes in mass from the start of the GRACE observation period were determined by calculating a cumulative sum of the mass rates calculated above.

3. Results

3.1. Monthly Precipitation and Temperature Grids

The gridded weather fields allow for the study of monthly time series at any location of interest. Alternately, they may be averaged or integrated over an area of interest. Referring to Figure 3, the southeastern and southcentral Alaska regions will be grouped into a GOA N (northern Gulf of Alaska) portion. The Canada region will be referred to as the GOA S (southern Gulf of Alaska) portion. Both the N and S watersheds have areas of 450,000 km^2. The GOA N watershed is roughly similar to the watershed used by *Wang et al.* [2004] and *Neal et al.* [2010] who reported values of 471,000 and 420,200 km^2, respectively. Figure 5 shows the monthly precipitation volumes into the northern and southern portions of the Gulf of Alaska watershed. The results show the strong annual cycle in precipitation as well as considerable interannual variability. The GOA N watershed receives, on average, 920 km^3 of water per year, and the GOA S watershed receives 700 km^3 annually.

The splines-with-tension method used to generate the gridded anomaly grids forces the surface through the station locations. As a result, the precipitation and temperature grids are guaranteed to match the station data. The cross validation tests described earlier provide one way of assessing the performance of the weather grids. For the test month considered, the correlation coefficient between the calculated and actual precipitation values was 0.93 and the root-mean-square error was 69 mm.

The annual variability in temperature is as expected, with a strong summer peak. In the GOA N watershed, the temperatures are consistently 2–3°C lower than in the GOA S watershed. Finally, the observed interannual variability in temperature is found to be much less than for precipitation.

3.2. Regression Analysis

Examples of calculated and measured runoff for individual basins are shown in Figure 6. Note that all of the time periods are different, based on station data availability. The respective Nash-Sutcliffe efficiencies are 0.72, 0.88, 0.83, and 0.87, indicating good overall agreement. The Nash-Sutcliffe efficiency [*Nash and Sutcliffe*, 1970] is calculated as

Figure 7. Monthly and annual runoff volumes for the GOA N and GOA S watersheds. (a and b) Monthly values for GOA N; (c) annual values for GOA N (closed symbols are the present study, open symbols are from *Wang et al.* [2004]); (d and e) monthly values for GOA S; (f) annual values for GOA S; (g) mean annual hydrographs for GOA N and GOA S. Bars in Figures 7c, 7f, and 7g show the estimated uncertainty in runoff.

$$NSE = 1 - \frac{\sum_{t=1}^{T}(Q_o^t - Q_m^t)^2}{\sum_{t=1}^{T}(Q_o^t - \overline{Q_o})^2}, \quad (6)$$

where the "*o*" and "*m*" subscripts indicate observed and modeled values, the summations are over the values in the time series and the overbar indicates the temporal mean. An NSE of 1 indicates a perfect model while an NSE of 0 indicates that the mean of the data is as good of a predictor as the model itself.

Time series of monthly runoff volumes and annual runoff totals derived from aggregation of all GOA N and all GOA S watersheds are shown in Figure 7. The mean annual runoff from the GOA N basin is found to be 792 ± 120 km^3, a number that is bracketed by the estimates of 725, 728, and 870 obtained by *Royer* [1982], *Wang et al.* [2004], and *Neal et al.* [2010]. This result produces a mean annual runoff depth of 1.76 m and an overall runoff ratio of 0.86. The mean annual runoff from the GOA S basin is found to be 538 km^3, which is consistent with the work of *Morrison et al.* [2012] and produces an overall runoff ratio of 0.77. The uncertainty bars in Figures 7c and 7f come from a weighted average of the mean absolute percent error between the predicted and measured mean annual discharges for the watersheds in Figure 6. This yields a value of 15%. A weighted average of mean absolute percent errors was also calculated for monthly flows and this is reflected in the uncertainty bars in Figure 7g.

The climatologies of precipitation and runoff shown in Figures 5e and 7g are as expected and reveal basic differences between the hydrology of the two regions. Both regions have peak precipitation in autumn (September–October). The GOA N region has peak runoff in the summer, indicating that the basin as a whole is dominated by summer snow and ice melt. The GOA S region has two distinct peaks, one in early summer (snowmelt) and one in late autumn (rainfall).

3.3. Water Balance

The methods described above provide *P*, *R*, and *ET* at a monthly time step. The common time period among these elements is 2000–2009. Over that time period, the mean annual *ET* of the GOAN watershed is 135.8 km^3. The maximum *ET* occurs during the month of July and the mean July value over that time period is 25.9 km^3.
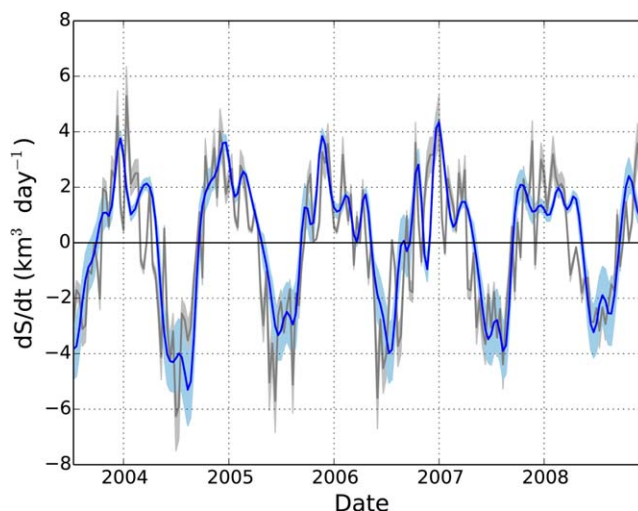
Figure 8 shows the rate of change in storage ($\frac{dS}{dt}$; equation (1)) from 2003 to 2009, which is the time period common between the above elements and the GRACE data. Uncertainty "envelops" are indicated by the shaded regions and were calculated using equation (1) of *Harmel et al.* [2009]. Note that for the GRACE data, a 20% error is assumed [*Arendt et al.*, 2013], a number that is discussed in detail in *Luthcke et al.* [2013]. It is clear that the satellite data agree generally well with the regression-based water balance ($r^2 = 0.61$, $p < 0.001$). The
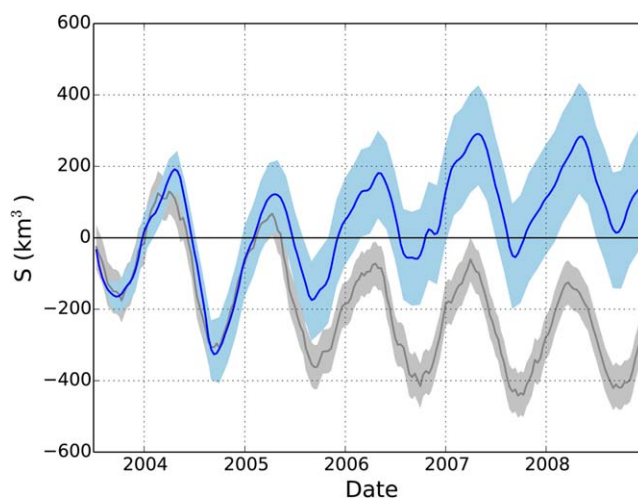
Figure 8. Changes in stored water of the GOA N region determined from GRACE gravimetry measurements (gray line) and modeled in this study (blue line). Shaded areas indicate uncertainty estimates.

data may also be presented as a time series of storage (i.e., a cumulative sum), which is shown in Figure 9. The uncertainty envelope grows with time for the regression-based model, following Equation (2) of *Harmel et al.* [2009]. For the cumulative GRACE data, the upper and lower envelops are adjusted so that if the linear trend were extracted from either of them, the result would be ±20% of the actual trend in the data.

The GRACE cumulative time series shows a multiannual trend toward mass loss (-57 ± 11 km^3 yr^{-1}) during the observation period. The v08 GRACE solution, which includes all hydrology, was used in this study and the linear trend in Figure 9, therefore, covers all multiannual changes in water storage in the domain. It is expected that the trend is dominated by GVL, but might also reflect other factors. In contrast to the loss shown by the GRACE data, the water balance model estimates show a slight gain in mass beginning in 2005. Seasonal losses, calculated as the difference between the maximum and minimum values of cumulative stored water (Figure 9) in a water year are shown in Figure 10.

4. Discussion

A direct comparison between the present runoff results and previous results is complicated by the different spatiotemporal resolutions of the studies. The work of *Wang et al.* [2004] is closest in this regard. Figure 7c provides a comparison of the annual GOA N discharges predicted by the two models and demonstrates that they are poorly correlated ($r^2 = 0.03$). Consideration of only the mean annual value allows for a comparison with *Neal et al.* [2010]. Their runoff depth of 1.86 m (excluding GVL) is very comparable to the present result of 1.76 m. This is intuitive due to the reliance of both studies on the PRISM climatology. *Neal et al.* [2010] used PRISM directly and the present study used it as the basis for the statistical downscaling procedure.

Figure 9. Cumulative changes in stored water of the GOA N region determined from GRACE gravimetry measurements (gray line) and modeled in this study (blue line). Shaded areas indicate uncertainty estimates.

The inclusion of the GRACE estimates in this study represents a significant step forward in terms of validation. Previous studies of GOA runoff have used various methods and data sources to arrive at discharge values but have not been able to provide an independent measurement due to incomplete coverage by stream gaging. The level of agreement observed in Figures 8 and 10 is a good validation of both estimates. The regression-equation approach is, by design, simple to implement and, therefore, accessible to a broad range of users. The GRACE data, largely due to their remotely sensed nature, demonstrate great potential
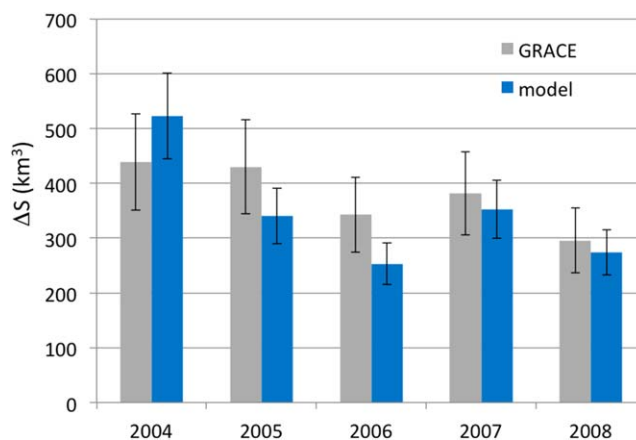
Figure 10. Seasonal loss in stored water. Error bars indicate uncertainty.

for water resources monitoring in regions where high-spatial-resolution in situ monitoring is prohibitive.

The divergence of the methods evident in Figure 9 and the fact that the water balance estimates generally underpredict seasonal losses (Figure 10) is a limitation of the ability of the regression-based approach to fully capture the enhanced runoff from watersheds containing retreating glaciers. Glaciers are formally included in the regression equations as a "percent snow and ice cover" land cover variable. Referring back to Table 1, the effect of glaciers can be observed. In summer months, the regression coefficient is positive, while in winter months it is negative. These trends capture the fact that glaciated watersheds store water in winter months and release it in summer months. The simplistic representation of glacier runoff in the regression equations has two main limitations. First, it is based only on precipitation in the current water year and temperature during the current month. Therefore, while it may be able to capture seasonal balances, it is not capable of simulating multiannual changes resulting from long-term removal of water stored in glacier ice. Second, the gaged watersheds, whose data informed the regression coefficients, tend to have limited glacier cover. Figure 11 shows glacier cover superimposed on the gaged watersheds and highlights the fact that glaciated areas are not substantially gaged. This data gap is particularly severe at the Southeast Alaska/Southcentral Alaska boundary.

Lacking a physically based approach to modeling the GVL contribution, one path forward is a superposition of a runoff volume from annual precipitation and a runoff volume from GVL estimates. This is precisely the strategy used by *Neal et al.* [2010]. Their 2.07 m runoff depth included 1.86 m from annual precipitation and 0.21 m from GVL. Their GVL is high, based on airborne laser altimetry data. The most recent GRACE data, clipped to the GOA N domain, suggest a long-term trend in runoff depth of 0.13 m yr^{-1}, which is assumed to be dominated by GVL. This GVL term combined with the regression model results yields an annual average GOA N runoff of 849 ± 121 m^3 yr^{-1}.
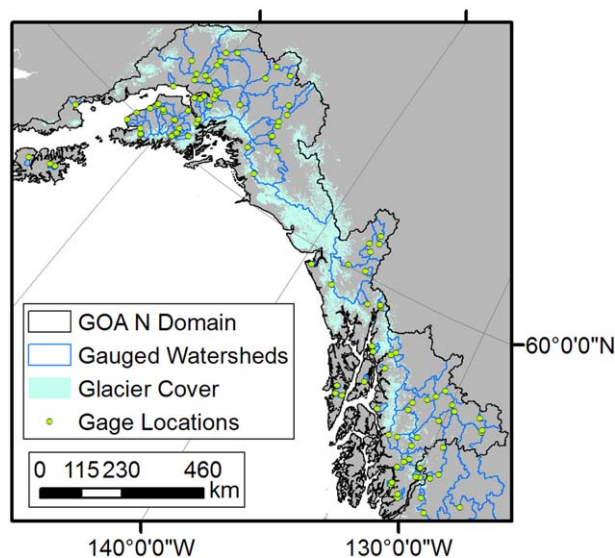

Figure 11. Glacier coverage from the Randolph glacier inventory (v.3.2) [*Pfeffer et al.*, 2014], gaged watersheds, gaging stations, and the GOA N domain.

5. Concluding Remarks

In summary, this study has produced several results of value to the continuing effort to improve runoff estimates for the Gulf of Alaska. As a preliminary step, high-resolution monthly weather grids were produced for Alaska, the Yukon Territory, and British Columbia. These grids are freely available from the NCDC. Second, regression equations for monthly flows were developed to (i) increase the spatiotemporal resolution of runoff estimates over previous studies and (ii) provide an easily accessible tool to a broad range of researchers interested in runoff (either local or GOA-wide) estimates. Future studies of GOA shelf circulation should

benefit from this increased spatial resolution and should help to identify the optimal resolution. The regression equations demonstrated good agreement with gage data and revealed a mean annual discharge for the GOA N region of 792 ± 120 km^3, which is a value bracketed by previous studies. While attention here has been paid to aggregated (GOA N domain) results, for the purposes of comparison to previous studies, recall that results are now easily obtained for any watershed of interest. The GOA S region was found to have a mean annual discharge of 538 ± 80 km^3.

Finally, this study provided a useful comparison between water storage estimates from a simple water balance (using terms determined herein) and from the GRACE project. It was found that the two methods agreed surprisingly well in terms of storage rates and seasonal changes. Longer term predictions of accumulated storage diverged due to accumulation of error in the regression-based water balance model and to inadequate representation of glacier processes in the model. The GRACE data suggest a GVL-dominated linear trend in runoff of 57 ± 11 km^3 yr^{-1} for the GOA N region, for a total value of 849 ± 121 km^3 yr^{-1}.

References

Arendt, A., K. Echelmeyer, W. Harrison, C. Lingle, and V. Valentine (2002), Rapid wastage of Alaska glaciers and their contribution to rising sea level, *Scienece*, *297*, 382–386.

Arendt, A., S. Luthcke, A. Gardner, S. O'Neel, D. Hill, G. Moholdt, and W. Abdalati (2013), Analysis of a GRACE Global Mascon Solution for Gulf of Alaska Glaciers, *J. Glaciol.*, *59*, 913–924.

Cleugh, H., R. Leuning, Q. Mu, and S. Running (2007), Regional evaporation from flux tower and MODIS satellite data, *Remote Sens. Environ.*, *106*, 285–304.

Curran, J., D. Meyer, and D. Tasker (2003), Estimating the magnitude and frequency of peak streamflows for ungaged sites on streams in Alaska and conterminous basins in Canada, *U.S. Geol. Surv. Water Resour. Invest. Rep.*, *03–4188*, 109 pp.

Dai, A., and K. Trenberth (2002), Estimates of freshwater discharge from continents: Latitudinal and seasonal variations, *J. Hydrometeorol.*, *3*, 660–687.

Daly, C., R. Neilson, and D. Phillips (1994), A statistical-topographic model for mapping climatological precipitation over mountainous terrain, *J. Appl. Meteorol.*, *33*, 140–158.

Daly, C., M. Halbleib, J. Smith, W. Gibson, M. Doggett, G. Taylor, J. Curtis, and P. Pasteris (2008), Physiographically sensitive mapping of climatological temperature and precipitation across the conterminous United States, *Int. J. Climatol.*, *28*, 2031–2064.

Etherington, L., P. Hooge, E. Hooge, and D. Hill (2007), Oceanography of Glacier Bay, Alaska: Implications for biological patterns in a glacial fjord estuary, *Estuaries Coasts*, *30*, 927–944.

Fowler, H., S. Blenkinsop, and C. Tebaldi (2007), Linking climate change modeling to impacts studies: Recent advances in downscaling techniques for hydrological modeling, *Int. J. Climatol.*, *27*, 1547–1578.

Gardner, A. S., et al. (2013), A reconciled estimate of glacier contributions to sea level rise: 2003 to 2009, *Science*, *340*, 852–857.

Glenn, E., P. Nagler, and A. Huete (2010), Vegetation index methods for estimating evapotranspiration by remote sensing, *Surv. Geophys.*, *31*, 531–555.

Guerschman, J., A. V. Dijk, G. Mattersdorf, L. Beringer, L. Hutley, R. Leuning, R. Pipunic, and B. Sherman (2009), Scaling of potential evapotranspiration with MODIS data reproduces flux observations and catchment water balance observations across Australia, *J. Hydrol.*, *369*, 107–119.

Harmel, R., D. Smith, K. King, and R. Slade (2009), Estimating storm discharge and water quality data uncertainty: A software tool for monitoring and modeling applications, *Environ. Model. Software*, *24*, 832–842.

Hermann, A., and P. Stabeno (1996), An eddy-resolving model of circulation on the western Gulf of Alasak shelf. 1—Model development and sensitivity analysis, *J. Geophys. Res.*, *101*, 1129–1149.

Hermann, A., D. Haidvogel, E. Dobbins, and P. Stabeno (2002), Coupling global and regional circulation models in the coastal Gulf of Alaska, *Prog. Oceanogr.*, *53*, 335–367.

Jacob, T., J. Wahr, T. Pfeffer, and S. Swenson (2012), Recent contributions of glaciers and ice caps to sea level rise, *Nature*, *482*, 514–518.

Jones, P. (1994), Hemispheric surface air temperature variations: A reanalysis and an update to 1993, *J. Clim.*, *7*, 1794–1802.

Luthcke, S., T. Sabaka, B. Loomis, A. Arendt, J. McCarthy, and J. Camp (2013), Antarctica, Greenland and Gulf of Alaska land-ice evolution from an iterated GRACE global mascon solution, *J. Glaciol.*, *59*, 613–631.

Marsh, R., D. Desbruyeres, J. Bamber, B. de Cuevas, A. Coward, and Y. Aksenov (2010), Short term impacts of enhanced Greenland freshwater fluxes in an eddy-permitting ocean model, *Ocean Sci.*, *6*, 749–760.

Mitchell, T., and P. Jones (2005), An improved method of constructing a database of monthly climate observations and associate high-resolution grids, *Int. J. Climatol.*, *25*, 693–712.

Morrison, J., M. Foreman, and D. Masson (2012), A method for estimating monthly freshwater discharge affecting British Columbia coastal waters, *Atmos. Ocean*, *50*, 1–8.

Mosier, T., D. Hill, and K. Sharp (2013), Very high resolution monthly climate surfaces with global land coverage, *Int. J. Climatol.*, *34*(7), 2175–2188.

Mu, Q., F. Heinsch, M. Zhao, and S. Running (2007), Development of a global evapotranspiration algorithm based on MODIS and global meteorology data, *Remote Sens. Environ.*, *111*, 519–536.

Mu, Q., L. Jones, J. Kimball, K. McDonald, and S. Running (2009), satellite assessment of land surface evapotranspiration for the Pan-Arctic domain, *Water Resour. Res.*, *45*, W09420, doi:10.1029/2008WR007189.

Mu, Q., M. Zhao, and S. Running (2011), Improvements to a modis global terrestrial evapotranspiration algorithm, *Remote Sens. Environ.*, *115*, 1781–1800.

Nash, J., and J. Sutcliffe (1970), River flow forecasting through conceptual models part i—A discussion of principles, *J. Hydrol.*, *10*, 282–290.

Neal, E., E. Hood, and K. Smikrud (2010), Contribution of glacier runoff to freshwater discharge into the Gulf of Alaska, *Geophys. Res. Lett.*, *37*, L06404, doi:10.1029/2010GL042385.

New, M., M. Hulme, and P. Jones (2000), Representing twentieth-century space-time climate variability. Part II: Development of 1901-96 monthly grids of terrestrial surface climate, *J. Clim.*, *13*, 2217–2238.

Pfeffer, W., et al. (2014), The Randolph Glacier Inventory (2014): A globally complete inventory of glaciers, *J. Glaciol.*, *60*, 537–552.

Ramillien, G., J. S. Famiglietti, and J. Wahr (2008), Detection of continental hydrology and glaciology signals from GRACE: A review, *Surv. Geophys.*, *29*, 361–374.

Royer, T. (1982), Coastal fresh water discharge in the northeast pacific, *J. Geophys. Res.*, *87*(C3), 2017–2021.

Royer, T., and C. Grosch (2006), Ocean warming and freshening in the northern Gulf of Alaska, *Geophys. Res. Lett.*, *33*, L16605, doi:10.1029/2006GL026767.

Sasgen, I., V. Klemann, and Z. Martinec (2012), Towards the inversion of GRACE gravity fields for present-day ice-mass changes and glacial-isostatic adjustment in North America and Greenland, *J. Geodyn.*, *59–60*, 49–63.

Simpson, J., G. Hufford, C. Daly, J. Berg, and M. Fleming (2005), Comparing maps of mean monthly surface temperature and precipitation for Alaska and adjacent areas of Canada produced by two different methods, *Arctic*, *58*, 137–161.

Swenson, S., and J. Wahr (2006), Estimating large-scale precipitation minus evapotranspiration from GRACE satellite gravity measurements, *J. Hydrometeorol.*, *7*, 252–270.

Wang, J., M. Jin, D. Musgrave, and M. Ikeda (2004), A hydrological digital elevation model for freshwater discharge into the Gulf of Alaska, *J. Geophys. Res.*, *109*, C07009, doi:10.1029/2002JC001430.

Weingartner, T. J., S. L. Danielson, and T. C. Royer (2005), Freshwater variability and predictability in the Alaska Coastal Current, *Deep Sea Res., Part II*, *52*, 169–191.

Wessell, P., and D. Bercovici (1998), Gridding with splines in tension: A green function approach, *Math. Geol.*, *30*, 77–93.

Wiley, J., and J. Curran (2003), Estimating annual high-flow statistics and monthly and seasonal low-flow statistics for ungaged sites on streams in Alaska and conterminous basins in Canada, *U.S. Geol. Surv. Water Resour. Invest. Rep., 03–4114*, 69 pp.

Zhang, K., J. Kimball, Q. Mu, L. Jones, S. Goetz, and S. Running (2009), Satellite based analysis of northern ET trends and associated changes in the regional water balance from 1983 to 2005, *J. Hydrol.*, *379*, 92–110.